Journal of Polymers and the Environment (2020) 28:1921–1933
https://doi.org/10.1007/s10924-020-01737-4

ORIGINAL PAPER

Effect of Zn-Cyclen Mimic Enzyme on Mechanical, Thermal and Swelling Properties of Cellulose Nanocrystals/PVA Nanocomposite Membranes

Muhammad Bilal Khan Niazi[1] · Zaib Jahan[1] · Arooj Ahmed[1] · Sikander Rafiq[2] · Farrukh Jamil[3] · Øyvind Weiby Gregersen[4]

Published online: 25 April 2020

Abstract
In this work, the effect of Zn-cyclen mimic enzyme on the properties of poly(vinyl alcohol)/cellulose nanocrystals (PVA/CNC) nanocomposite membranes have been studied at three different relative humilities (0%RH, 53%RH and 93%RH). Different amounts of mimic enzyme were incorporated, and membranes were prepared by solution casting. The fabricated nanocomposite films were characterized by X-ray Diffraction, Fourier Transform Infrared Spectroscopy and Scanning Electron Microscopy. The results revealed good interfacial interactions between the constituents. The membranes showed enhanced uptake of moisture, with increasing mimic enzyme concentration as well as humidity. The membranes demonstrated the ability to uptake moisture for almost 4 days. The mechanical properties showed an opposite trend as expected. Tensile strength, tensile modulus and dynamic mechanical properties declined with increase in humidity along with mimic enzyme amount. The highest elastic modulus i.e. 33 MPa was found at the lowest humidity i.e. 0%RH for the pure PVA membrane. Similarly, the maximum tensile strength of 118 MPa was found at the similar conditions for the same formulation. The obtained results suggested the potential application of PVA/CNC and mimic enzyme membranes in CO_2 separation.

✉ Muhammad Bilal Khan Niazi
m.b.k.niazi@scme.nust.edu.pk

[1] Department of Chemical Engineering, School of Chemical and Materials Engineering, National University of Sciences and Technology, Islamabad, Pakistan

[2] Department of Chemical Polymer and Composite Material Engineering, University of Engineering and Technology, Lahore Campus, Pakistan

[3] Chemical Engineering Department, COMSATS University Islamabad, Lahore Campus, Pakistan

[4] Department of Chemical Engineering, Norwegian University of Science and Technology, Trondheim, Norway

Graphic Abstract

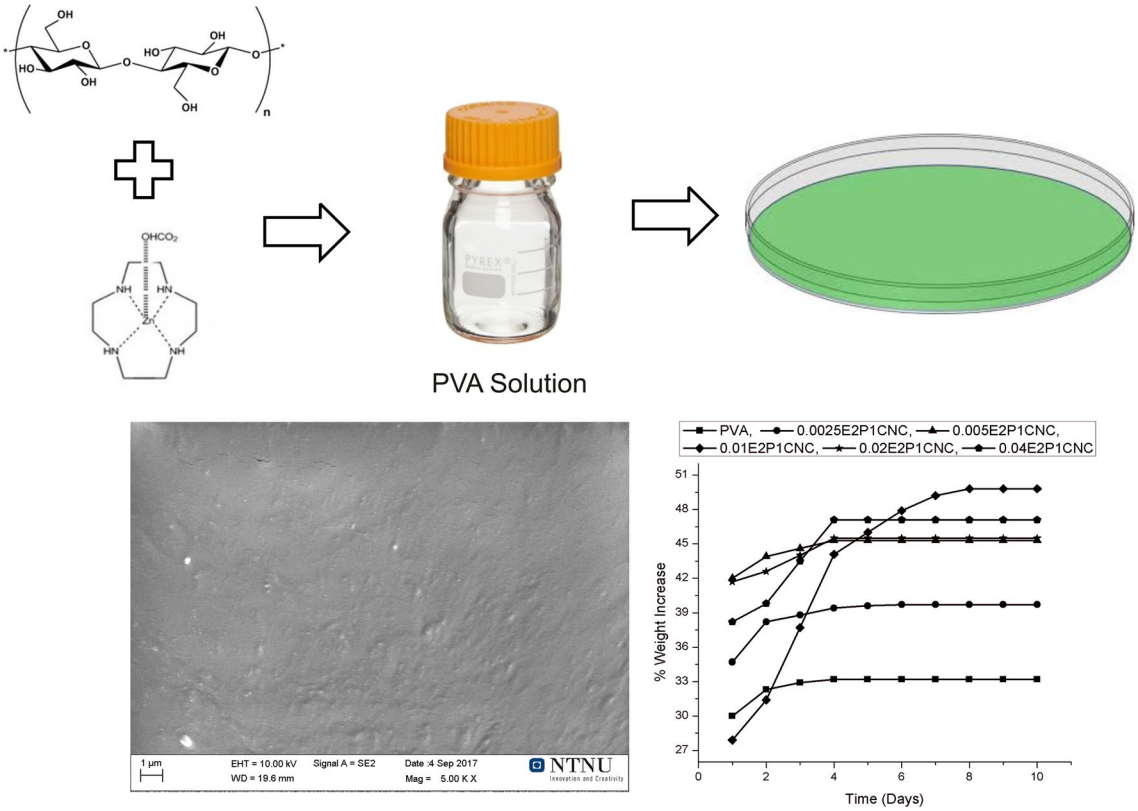

Keywords Zn-cyclen mimic enzyme · Poly(vinyl alcohol) · Mechanical strength · Dynamic mechanical properties · Thermogravimetric analysis

Introduction

Credited to low consumption of energy, ability to operate continuously, ease of upscaling and hybridization [1], membranes have gained significant importance in the field of chemical technology. They have successfully been used in a wide range of applications. These applications include but are not limited to controlled drug delivery [2], separation processes, packaging [3], waste water treatment [4], gas separation [5], pervaporation [6], reverse osmosis [7]. Amongst the biological and synthetic membranes, the polymeric synthetic membranes have been a huge area of interest for the researchers because of the easiness of tailoring their properties. Polymeric composites have been extensively investigated during the last six decades, with the objective of enhancing their characteristics [8]. The unavoidable problem associated with polymers is their inadequate mechanical strength [9], that limit their usage. To overcome this issue, they have been blended with various kinds of fillers that act as reinforcement improving mechanical, swelling and thermal properties. Fillers that is derived from petroleum based substances have upstretched environmental concerns. These are non-biodegradable, causes damage to oxygen demand [10], landfills and septic systems [11]. Moreover, the fluctuating oil prices is an additional problem [12]. This inflicts stern economic burden on the society. Consequently, a prevalence of naturally derived fillers has been observed. This shift has levied a substantial challenge to the researchers and scientists to develop those fillers that have no harmful impact on human health and environment. Furthermore, the fillers should be non-toxic and economical at the same time.

Different polymers like poly(ethylene) (PE) [13], poly(styrene) (PS) [14], poly(urethane) (PU) [15], poly(caprolactone) (PCL) [16], poly(propylene) (PP) [17], poly(β-hydroxy octanoate) (PHO) [18] etc., have been reinforced utilizing various fillers. Among these polymers, poly(vinyl alcohol) (PVA) has the privilege of being biocompatible, biodegradable [19], non-toxic, hydrophile [20], water soluble, inexpensive and environmental friendly [21]. All these characteristics render PVA as an ideal choice to utilize in diverse applications. But PVA has two major drawbacks, firstly in wet conditions, it shows poor strength and

stiffness and secondly its mechanical properties get weakened with increasing temperature [22]. To alleviate these downsides, PVA has been blended with fillers like cadmium sulfide [23], silica [24], carbon nanotubes [25], zeolite immedazolite frame works [26], ZSM-5 [27], hydroxyapatite [28], gold [29], silver [30], and iron oxide [31]. But their processability, recyclability, biocompatibility and biodegradability are much less than their organic counterparts. For this reason, reinforcement agents that are organic in nature are given preference and renewable sources are continuously explored.

Owing to their biocompatibility, biodegradability, cost-effectiveness, non-toxicity, antioxidant and antimicrobial activity and ease of functionalization, natural polymers like chitosan [32], alginate [33], starch [34], gelatin [35], fibrin [36] and lignin [30] have been studied as fillers. Cellulose is one of the natural polymers that entail all these attributes. Not only it is the most abundant organic polymer [12, 37] but is also renewable [37] derived primarily from plant sources and is thus, inexhaustible. Also, it is inexpensive, has low density and is environmentally safe [38]. The extraction of cellulose is a relatively cheap process. Nanocellulose is considered as "the choice of sustainable materials in the twenty-first century" [39, 40]. Cellulose nanocrystals (CNCs) or whiskers have phenomenal mechanical properties and is therefore has a great deal of interest to be incorporated into polymeric matrixes. Cellulose crystals have been reported to have the elastic modulus of 168 GPa [40] and 143 GPa for tunicin whiskers [37], which is far better than that of glass fibers i.e., 73 GPa [41]. Beside enhancing the mechanical properties, CNC reinforces thermal, swelling, barrier and permeability properties. Moreover, it has high aspect ratio and low density [41]. For CO_2 separation, the facilitated transport carrier membranes should exhibit high selectivity as well as CO_2 permeance.

To further improve the CO_2 permeability properties, mimic enzymes can be incorporated to fabricate facilitated transport membranes. A substance that has the tendency to mimic the natural mimic enzymes is an ideal choice for this purpose. A special type of facilitated transport carrier membranes is enzymatic membranes that contain naturally occurring mimic enzymes and mimic the natural respiratory system of human beings. This phenomenon is expected to achieve more success in future for CO_2 capturing [42]. The limited lifespan, high cost and highly sensitive to impurities, temperature and pH are the obstacles in the scaling up of this technology [43]. Many metal complexes have this ability, among them zinc (Zn) has been reported to have highest activity [42, 44]. The main effect of the mimic enzyme and the biological mimic enzyme is to act as a catalyst enhancing the speed of the $CO_2 + H_2O$ to CO_3H- reaction. Incorporation of a mimic enzyme may improve the swelling ability, consequently improving the affinity for certain gases. So, the facilitated transport membranes designed from PVA, CNC and mimic enzyme have the propensity to be used in gas separation.

Keeping this in mind, a facilitated transport membrane was fabricated with PVA as a polymer matrix, CNC as reinforcement and zinc cyclen mimic enzyme to enhance barrier and permeability properties. X-ray Diffraction (XRD) was carried out for phase identification. Fourier Transform Infrared (FTIR) Spectroscopy was employed to study the interaction between the functional groups. Scanning Electron Microscopy (SEM) was done to study the membrane structure. The mechanical properties were explored by tensile testing and dynamic mechanical analysis (DMA). Thermal gravimetric analysis (TGA) and Differential scanning calorimetry (DSC) revealed the thermal stability of the prepared nanocomposites.

Experiments

Materials

Poly(vinyl alcohol) ($M_W = 89{,}000–124{,}000$ and 87–89% hydrolyzed), crystalline nanocellulose (CNC) (average length $= 130 \pm 67$ nm, average width $= 5.9 \pm 1.8$ nm and aspect ratio $= 23 \pm 12$ nm [49]), Zinc perchlorate hexahydrate $Zn(ClO_4)_2$, 1,4,7,10-tetraazzacyclododecane and absolute alcohol were purchased from Sigma Aldrich. Distilled water was used for the synthesis purpose.

Methods

Synthesis of Mimic Enzyme (Zn-Cyclen)

The mimic enzyme (Zn-cyclen) was synthesized by the method reported in literature [45]. Cyclen was dissolved in 5 ml absolute ethanol with subsequent addition of $Zn(Cl_4O)_2$ and stirring for 1.5 h. Afterwards, it was extracted by vacuum filtration and washed with ethanol several times.

Fabrication of PVA, CNC and Mimic Enzyme Nano composite Membrane

2 g PVA was dissolved in distilled water and was stirred for 3 h at 90 °C The solution was left rolling overnight. 0.02 g of CNC suspension was poured into the PVA solution. Then, the desired amount of mimic enzyme was added (See Table 1). The solution was mixed and stirred well. The resulting homogeneous suspension was casted into polypropylene petri dishes. The mixture was left for atmospheric drying.

Table 1 Materials code and corresponding concentration of CNC and mimic enzyme

Formulations	PVA (g)	CNC (g)	Mimic enzyme (g)
PVA	2	–	–
PCNC1	2	0.002	–
0.0025E2PCNC1	2	0.002	0.0025
0.005E2PCNC1	2	0.002	0.005
0.01E2PCNC1	2	0.002	0.01
0.02E2PCNC1	2	0.002	0.02
0.04E2PCNC1	2	0.002	0.04

Characterization

Fourier Transform Infrared Spectroscopy (FTIR)

The FTIR spectra of all the prepared formulations was recorded in the range of 800–4000 cm^{-1} by the Thermo Nicolet Nexus FTIR spectrometer equipped with attenuated total reflectance (ATR). The shifts in intensities were studied as the basis of interactions between PVA, CNC and mimic enzyme.

Swelling

The swelling percentage of the prepared nanocomposite membranes was analyzed gravimetrically at 53 and 93% relative humidities (RH). The measurements were taken continuously for ten days. Swelling was then calculated by following equation:

$$\text{Swelling}(\%) = \frac{W_n - W_o}{W_o} \times 100 \quad (1)$$

where W_n represents the weight at the day of measurement (mg) and W_o represents initial weight (mg).

X-Ray Diffraction (XRD)

For phase identification and studying the crystalline behavior of the formulated membranes Bruker D8 Focus X-ray Diffractometer equipped with alynxEye™ super speed detector was employed. The wavelength of Cu-radiation was 1.5418 Å. The specimen was scanned at 2θ varying between 10° and 50°, at a step size of 0.02° and scan speed of 2 s per step. The equipment was operated at the current and voltage of 40 mA and 40 kV, respectively.

Scanning Electron Microscopy (SEM)

For morphological analysis of the membranes, Hitachi SEM SU 3500 (Japan) operated at the voltage of 5 kV was used. Prior to analysis, the specimen was sputter-coated with a thin layer of gold. This was done to avoid the accumulation of charge on the surface of the membranes. For cross-sectional analysis, the specimen was first freeze using liquid nitrogen and then instantly cracked. The cross-section was also sputter coated with a thin gold layer.

Thermal Analysis

Thermogravimetric Analysis (TGA)

A thermogravimetric analyzer (TGA, Q500, Thermal) was used for investigating the thermal stability of the nanocomposite membranes. For this purpose, samples weighing 8–10 mg were placed in an open aluminum pan and heated at a rate of 10 °C/min. The heating was carried out from room temperature to 700 °C. The results are reported as percentage weight loss as a function of temperature.

Differential Scanning Calorimetry (DSC)

Differential Scanning Calorimetry (DSC, TA Q100, Thermal Scientific) was employed to investigate the glass transition temperature (T_g), cold crystallization and melting temperature. A sample weighing 10 g was placed in aluminum pan and covered properly. An empty pan was chosen as a standard. The analysis was carried out under nitrogen atmosphere at a rate of 10 °C/min, while the temperature was varied from 30 to 250 °C After initial heating, the specimen was cooled and then a second scanning was performed.

Mechanical Properties

Mechanical Testing

For investigating the mechanical properties, Zwick Roell Tensile Testing equipment was used. The properties like tensile strength (TS), Elongation at Break (EB) and Elastic Modulus were determined. The analysis was performed in accordance to ASTM D638 at ambient conditions. The length and width of the sample was 50 mm and 15 mm, respectively and thickness was 0.1 ± 0.02 mm. The cross head speed was 50 mm/min. All the properties were evaluated at 0%RH, 53%RH and 93%RH. Before analyzing, the specimen was conditioned for four days. All the measurements were carried out five times.

Dynamic Mechanical Analysis

The dynamic mechanical behavior of the nanocomposite membranes was investigated using a Dynamic Mechanic Analyzer 242 (NETZSCH-Geratebau GmbH) equipped with liquid nitrogen cooling system. The investigation was carried out at a constant frequency of 1 Hz, heating rate of 2 °C/min and temperature was varied between − 20 and 120 °C. The sample dimensions were as follows: length 20 mm, width 5 mm and 0.1–0.2 mm thickness. The specimen was conditioned for four days and dynamic mechanical behavior was estimated at 0%RH, 53%RH and 93%RH.

Results and Discussion

Fourier Transform Infrared Spectroscopy

The FTIR spectrum elucidates the chemical interactions between polymer, cellulose nanocrystals and mimic enzyme. The FTIR spectrum of the pure PVA membrane (without CNC and mimic enzyme) shows a broad band near 3350 cm^{-1}, which is due to the stretching vibration of free –OH groups. The peak arising at 2900 cm^{-1} is ascribed to the aliphatic stretching of alkyl groups. The characteristic peak of PVA observed at 1150 cm^{-1}, owes its presences due to stretching of –C–O functional group. This band is considered as the criterion for the crystallinity of PVA [46]. For the formulation incorporating CNC and mimic enzyme, all the peaks mentioned above were observed in the FTIR spectrum with a slight shift in peak intensity. The shift in peak intensity was considered as a basis of the interactions between PVA and mimic enzyme. The intensity of band at 3350 cm^{-1} was reduced. This reduction was an indication of the formation of stronger bonds between PVA and mimic enzyme. The band at 2900 cm^{-1} indicates the intermolecular hydrogen bonding between the polymeric chains. A sharp peak arising at 1750 cm^{-1} is attributed to the residual acetate groups present in PVA. After the addition of mimic enzyme, the intensity of this peak reduced substantially. This again confirms the hydrogen bonding interactions among the constituents used for the fabrication of nanocomposite membranes. The intensity of the peak appearing at 1420 cm^{-1} also decreased, this peak is due to the bending vibrations of –CH. At 800 cm^{-1} the appearance of peak is credited to the pyranose ring. In the spectra of PVA/CNC and mimic enzyme, shown in Fig. 1, all the characteristic peaks of the constituents are present. With an increase in mimic enzyme concentration, the peaks shifted accordingly. This demonstrated the successful interactions between polymer, CNC and mimic enzyme and also the successful incorporation of mimic enzyme into the polymer matrix.

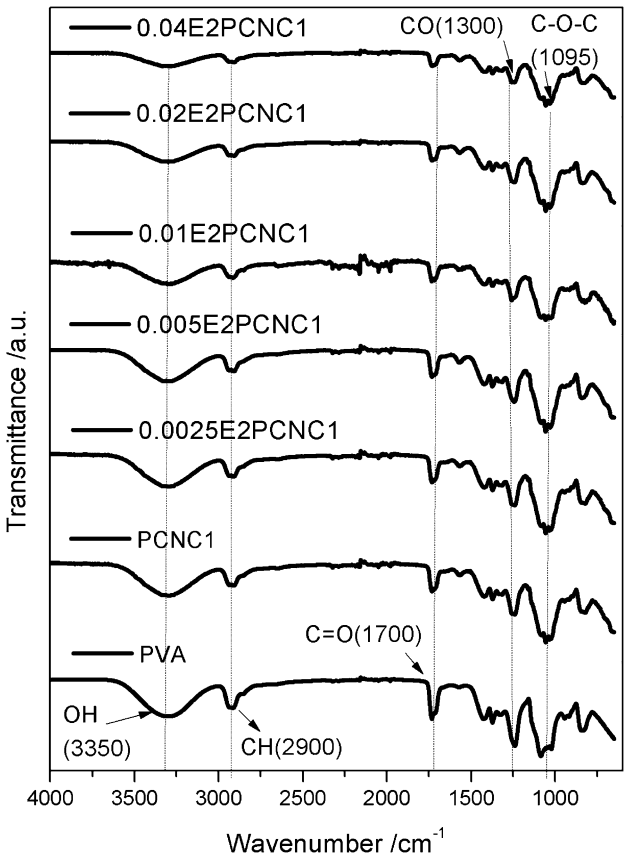

Fig. 1 FTIR spectra of PVA, PCNC1 and PVA/CNC/Mimic enzyme nanocomposite membranes

Swelling

For evaluating the swelling ability of the nanocomposite membranes, the behavior was analyzed after a step change in RH from 0%RH to 53%RH or 93%RH. Figure 2a, b shows the swelling as a function of time. The swelling of PCNC1 membrane was 4.5% and equilibrium was attained after 3 days, as reported in our previous study [47]. After the incorporation of mimic enzyme, swelling showed an abrupt increase. But the values were still higher than those membranes without mimic enzyme. The swelling of all the formulations increased with increase in time. Each sample attained equilibrium at a different day. The maximum ability to uptake moisture was depicted by the specimen with 0.04 g of mimic enzyme. The swelling was 7.9% and equilibrium was attained at 4th day. Roughly, all the samples achieved equilibrium at 4th or 5th day. But the sample with 0.005 g mimic enzyme achieved equilibrium on 6th day. Among all the samples, the sample without CNC and mimic enzyme (i.e., pure PVA) showed lowest swelling ability of 3.4%.

At 93%RH, a drastic improvement in swelling ability was observed. All the formulations at 93%RH displayed a quicker increase in swelling as a function of time. But

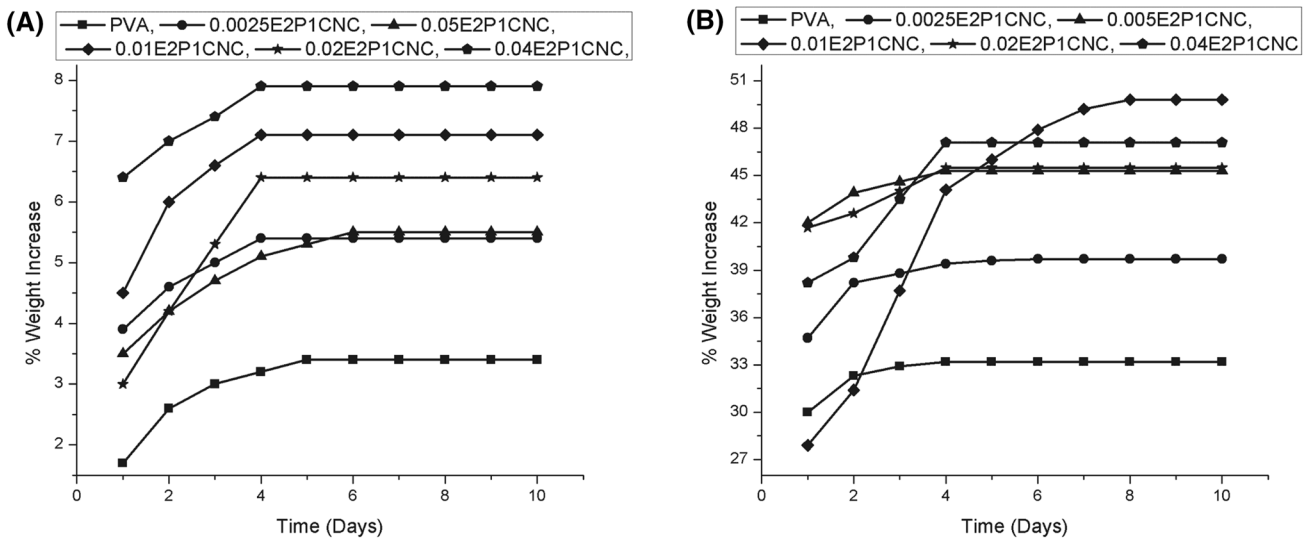

Fig. 2 Moisture Uptake of PVA and PVA/CNC/Mimic enzyme nanocomposite membranes at **a** 53%RH, **b** 93%RH

the trend here also was irregular. As compared to PCNC1 (without mimic enzyme) the value increased after inclusion of mimic enzyme. The swelling ability of PCNC1 was 30% and it increased to 39.7%, when 0.0025 g mimic enzyme was added. As the mimic enzyme concentration was increased gradually to 0.005 g and 0.01 g, the swelling increased to 45.3% and 49.8%, respectively. With the further increase to 0.02 g the swelling reduced to 45.5% and then again increased to 47.1% at 0.04 g mimic enzyme concentration. All the nanocomposite membranes achieved equilibrium at 4th day, except 0.0025E2PCNC1 and 0.01E2PCNC1. The maximum ability to uptake moisture of 49.8% was depicted by 0.01E2PCNC1. Moreover, this formulation attained equilibrium at 8th day.

The results evidently illustrate that the addition of mimic enzyme has improved the swelling capability of the PVA membranes. It also suggests positive effect on solubility of water in PVA matrix, that ultimately enhanced the moisture retention [45].

To be utilized for CO_2 separation, it is important to have high swelling ability at high humidity [47]. So, the formulations entailing PVA, CNC and mimic enzyme are well suited for the suggested application.

X-Ray Diffraction

To explore the crystalline structure of the prepared nanocomposite membranes, the XRD analysis was carried out at 0%RH, 53%RH and 93%RH and results are shown in Fig. 3a–c.

At 0%RH, two peaks were observed in the diffractogram. PVA is normally characterized by strong peaks, appearing at 19.8° and 22.76°. These peaks unveil the semi crystalline nature of PVA [48]. The peak appearing at 22.76° is one of the peaks of nanocellulose [37]. The other characteristic peaks of nanocellulose, appearing in amorphous halo at 15.5° and 16.5° were not found. The disappearance of these peaks may be due to the addition

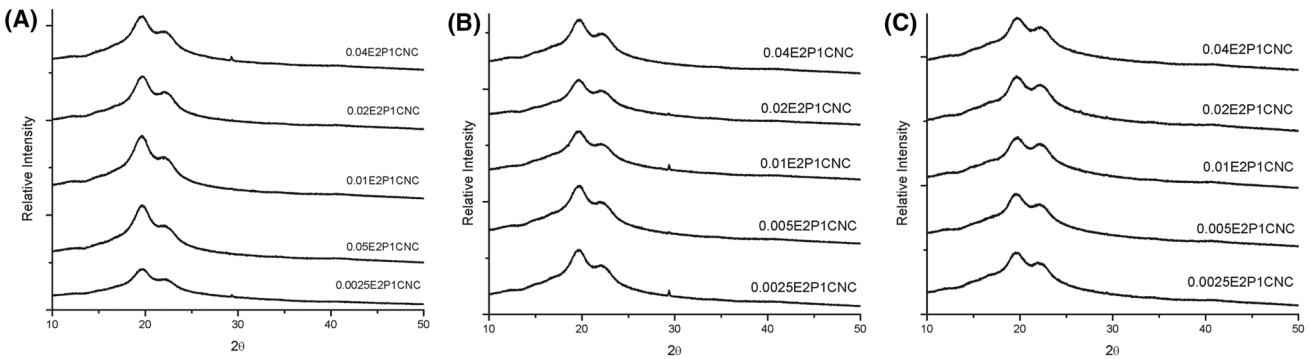

Fig. 3 XRD patterns of PVA/CNC/Mimic enzyme nanocomposite membranes at **a** 0%RH, **b** 53%RH, **c** 93%RH

of mimic enzyme that causes the change in crystallinity. Furthermore, the addition of mimic enzyme caused intermolecular interference among the polymer chains and promotes hydrogen bonding interactions [49]. As the mimic enzyme concentration increased, the intensity of peak pertaining to PVA increased. Similar patterns were observed at 53%RH and 93%RH.

Scanning Electron Microscopy

The surface morphology and cross-sectional images of pure PVA membrane, PCNC1, 0.01E2P1CNC, 0.04EP1CNC nanocomposite membranes are shown in Fig. 4.

All the prepared nanocomposite membranes were dense in nature. A homogenous and smooth morphology of pure PVA membrane was observed, this was due to the hydrophilic nature of PVA that aided in formation of smooth surface. At PCNC1, smaller and larger clusters of cellulose

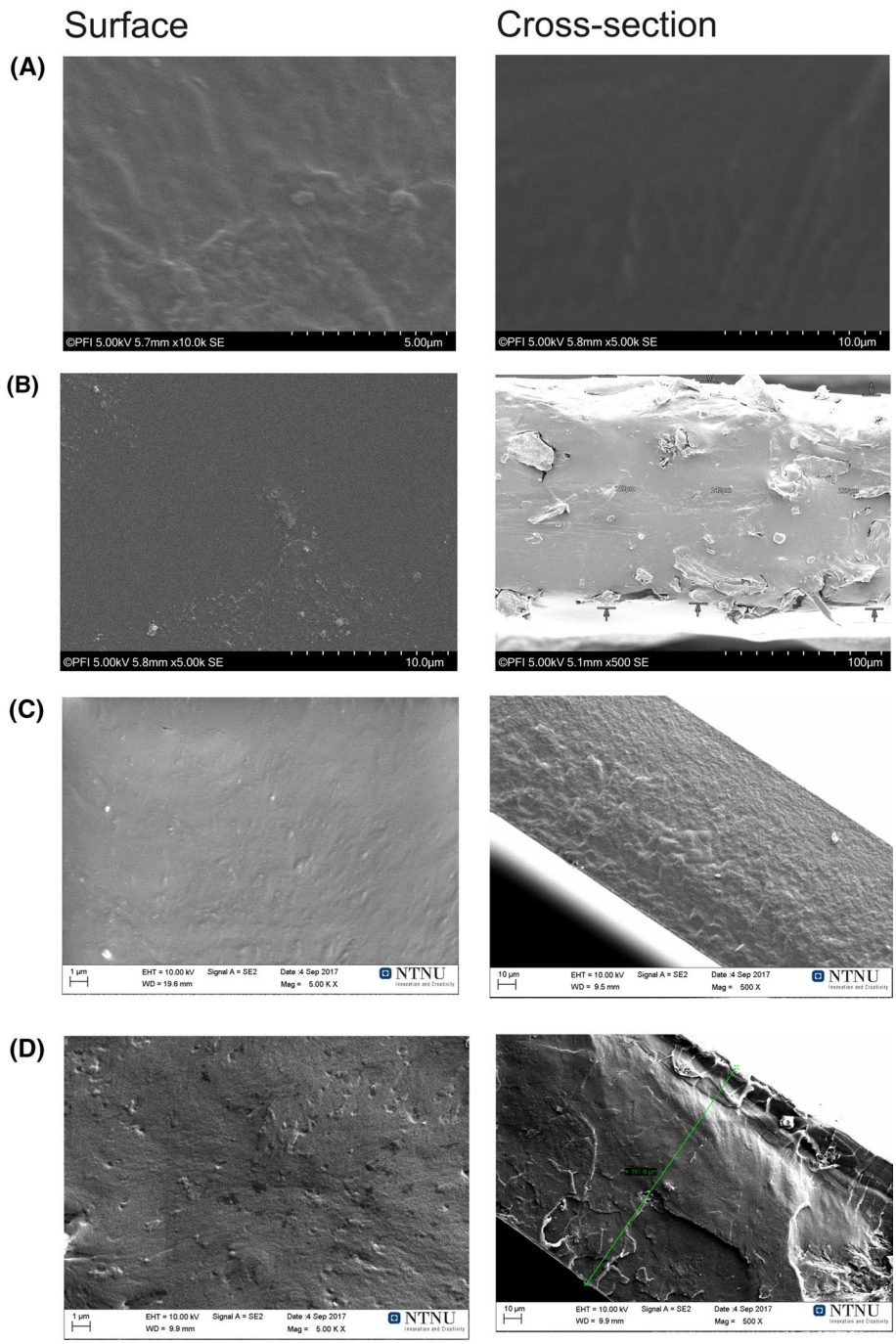

Fig. 4 SEM surface and cross sectional images of **a** PVA, **b** PCNC1, **c** 0.01E2P1CNC, **d** 0.04EP1CNC nanocomposite membranes

nanocrystals can be seen distributed throughout the thickness of the membrane. With the addition of CNC, the surface became rough. After the addition of mimic enzyme to PVA/CNC, the surface became rougher. However, the dispersion and distribution of cellulose nanocrystals seems more uniform with addition of mimic enzyme.

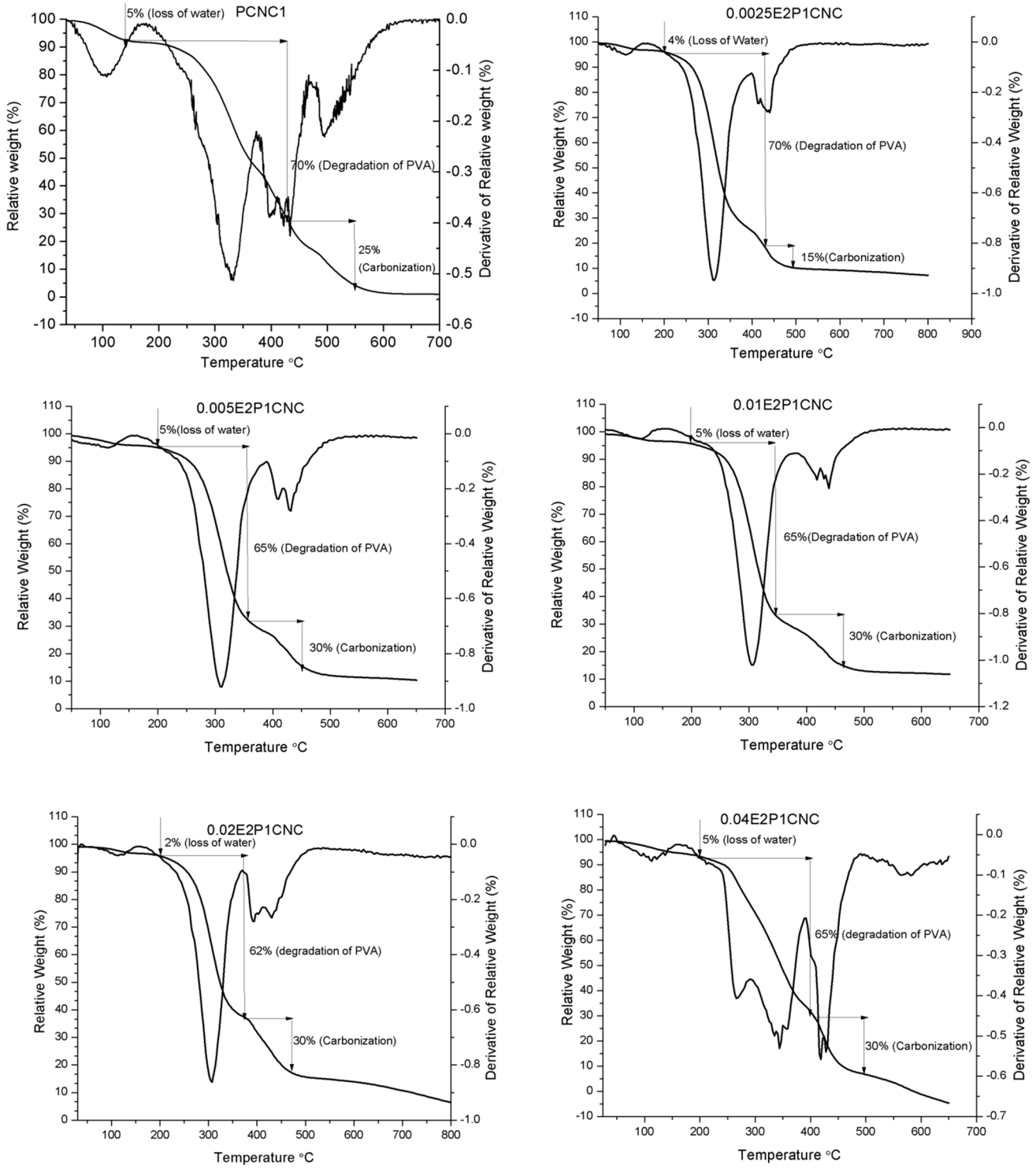

Fig. 5 TGA and DTGA curves of PVA/CNC1 and PVA/CNC/Mimic enzyme nanocomposite membranes

Thermal Analysis

Thermogravimetric Analysis (TGA)

The thermal gravimetric analysis is shown in Fig. 5. The percentage weight loss is reported as a function of temperature. The three degradation stages can be clearly observed in all the thermograms [49, 50]. The behavior of weight loss curves was quite similar for all formulations. In the first degradation stage, ranging from 80 to 130 °C is associated with the weight loss occurring due to loss of water. The rate of evaporation was found to be increasing with a gradual increase in the mimic enzyme content. It was observed that, the thermal stability was directly related to the amount of mimic enzyme in the nanocomposite membranes. In the subsequent stage, 150 to 350 °C, the weight loss occurred due to degradation of polymer chain. This loss is chiefly associated with the dehydration of hydroxyl groups and subsequent formation of aliphatic and low molecular unsaturated carbon species [51]. The last degradation stage, after 400 °Cis due to the carbonization of the constituents present in the nanocomposite membrane (Fig. 5).

According to the TGA curves, most of the degradation occurs in the temperature range of 250 to 400 °C. Approximately 70% of the weight loss occurs during this phase. The first three formulations with 0.0025 g, 0.005 g and 0.01 g mimic enzyme had no significant effect on the thermal stability of the nanocomposite membranes. Nevertheless, the stability increased at 0.02 g and 0.04 g mimic enzyme concentration, particularly at 0.04 g mimic enzyme content.

Differential Scanning Calorimetry (DSC)

DSC analysis comprised of heating, cooling and again heating cycle. The information about glass transition temperature, crystallization temperature and melting temperature was revealed from DSC analysis as shown in Fig. 6. No generalized trend was observed in glass transition temperature T_g of PVA/CNC nanocomposite membranes after the addition of mimic enzyme was observed. Initially, T_g increased with the gradual increase in mimic enzyme content except at 0.005 g. The T_g of PCNC1 nanocomposite membrane was 66 °C. The T_g increased to 78 °C at 0.0025 g mimic enzyme and then decreased to 70 °C. After that, it increased to 78 °C, 78.3 and 79 °C at 0.01 g, 0.02 g and 0.04 g mimic enzyme amount.

Similarly, no drastic effect on the melting temperature was detected with increase in amount of mimic enzyme. The melting point of all the formulations was approximately 230 °C except for the 0.0025 g mimic enzyme. In that case, melting point was 238 °C.

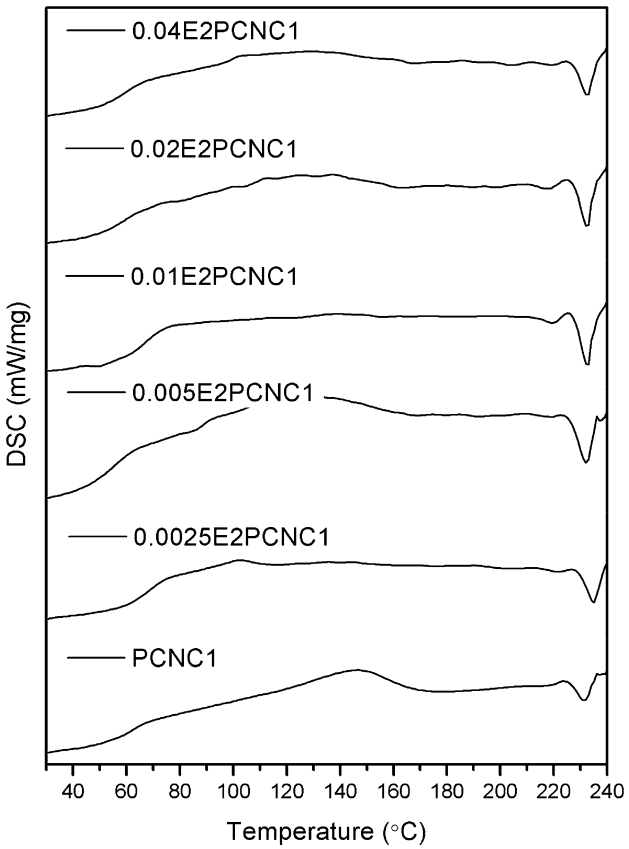

Fig. 6 DSC curves for PVA/CNC and PVA/CNC/Mimic enzyme nanocomposite membranes

Mechanical Properties

Mechanical Testing

Mechanical properties of the nanocomposite membranes loaded with varying mimic enzyme content were evaluated at 0%RH, 53%RH and 93%RH and results are shown in Fig. 7a–c. At 0%RH, the tensile strength of the membranes decreased after the incorporation of mimic enzyme and nanocellulose crystals, as compared to pure PVA membrane. The tensile strength decreased till 0.01 g mimic enzyme loading, then it increased with the increase in mimic enzyme content to 0.02 g and decreased again at 0.04 g mimic enzyme concentration. A similar trend was observed at 53%RH and 93%RH. As the relative humidity was increased, the tensile strength decreased. The maximum tensile strength of 70 MPa was achieved at 0%RH for the formulation 0.0025E2PCNC1. The same composition attained the tensile strength of 40 MPa and 7 MPa at 53% and 93%RH. At 93%RH the elastic modulus was found to be higher than the pure PVA membranes, which confirms that membranes have significant potential to be used at higher humidities.

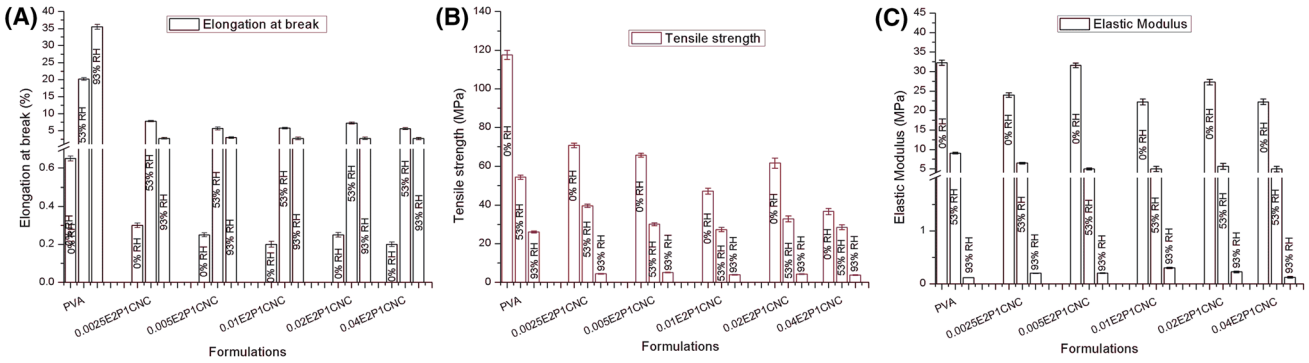

Fig. 7 Mechanical Properties of PVA/CNC/Mimic enzyme nanocomposite membranes at 0%RH, 53%RH, 93%RH **a** Elastic modulus, **b** Elongation at break and **c** Tensile Strength

The tensile modulus also displayed a similar trend as tensile strength. This may be due to the reason that failure strength of the polymer matrix is greater than that of the mimic enzyme. The obtained results were found in agreement with the literature [37].

The highest elongation at break was depicted at 53%RH. The highest value of 9% was shown by the formulation 0.0025E2PCNC1. With the increase in mimic enzyme content, the elongation at break decreased slightly.

Dynamic Mechanical Analysis

To explore the thermomechanical properties, Dynamic Mechanical Analysis were performed at 0%RH, 53%RH and 93%RH. Figure 8a shows the results of storage modulus E' versus temperature. No organized change in DMA was observed with the addition of mimic enzyme. At 0%RH, the sample with 0.05 g mimic enzyme showed the highest mechanical strength followed by 0.025 g mimic enzyme. For rest of the specimen, namely 0.01E2P1CNC, 0.02E2P1CNC and 0.04E2P1CNC the storage modulus decreased with the gradual increase in mimic enzyme content. The obtained results suggest the occurrence of mechanical percolation phenomenon, which occurred as a result of hydrogen bonding interactions [52]. As the humidity was increased further, a decrease was observed in dynamic mechanical strength.

The damping properties of the nanocomposite membranes was evaluated by measuring tan delta (tan δ). Tan δ as a function of temperature is shown in Fig. 8c. The formulation 0.005E2P1CNC shows the highest value of tan δ and it decreased with the increase in mimic enzyme concentration. The obtained results were in line with the tensile strength results. As the tensile strength decreased, it decreased the storage modulus which ultimately resulted in an increase in tan δ.

Conclusions

The objective of this study was to explore the mechanical, swelling and thermal properties of the PVA/CNC nanocomposite membranes incorporating Zn-cyclen mimic enzyme. PVA and CNC were taken constant as 2 g and 0.02 g, respectively. Whereas, Zn-cyclen mimic enzyme was varied as 0.0025 g, 0.005 g, 0.01 g, 0.02 g and 0.04 g. DMA, TGA, DSC and swelling resulted suggested that the prepared nanocomposite membranes can be utilized in CO_2 separation. The inclusion of mimic enzyme enhanced the swelling properties with the increase in humidity. Swelling increased with humidity for all formulations. The addition of mimic enzyme also increased the crystallinity of the membranes. But it has negative effect on the tensile strength, elongation at break, elastic modulus and dynamic mechanical properties. Consequently, tan δ increased with increase in mimic enzyme concentration. The nanocomposite membranes entailing PVA/CNC/Mimic enzyme can be successfully used in gas separation particularly CO_2 separation.

Fig. 8 Dynamic mechanical analysis curves of PVA/nanocellulose composite membranes at **a** Storage modulus and tan δ at 0%RH, **b** Storage modulus and tan δ at 53%RH, and **c** Storage modulus and tan δ at 93%RH

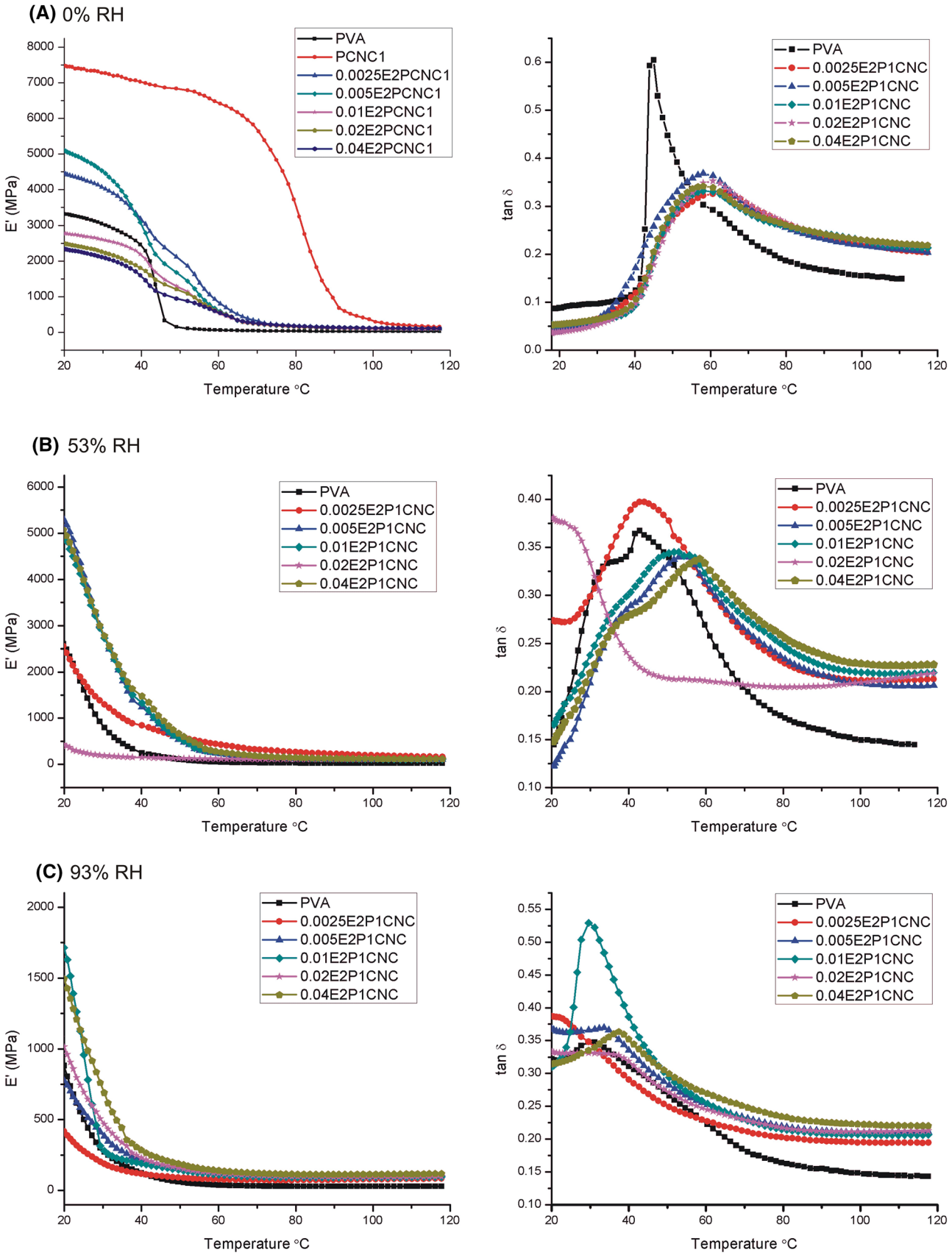
(A) 0% RH
PVA
PCNC1
0.0025E2PCNC1
0.005E2PCNC1
0.01E2PCNC1
0.02E2PCNC1
0.04E2PCNC1
E' (MPa)
tan δ
Temperature °C
(B) 53% RH
PVA
0.0025E2P1CNC
0.005E2P1CNC
0.01E2P1CNC
0.02E2P1CNC
0.04E2P1CNC
E' (MPa)
tan δ
Temperature °C
(C) 93% RH
PVA
0.0025E2P1CNC
0.005E2P1CNC
0.01E2P1CNC
0.02E2P1CNC
0.04E2P1CNC
E' (MPa)
tan δ
Temperature °C

References

1. Mulder M (2012) Basic principles of membrane technology. Springer Science & Business Media, New York
2. Stamatialis DF, Papenburg BJ, Girones M, Saiful S, Bettahalli SN, Schmitmeier S, Wessling M (2008) Medical applications of membranes: drug delivery, artificial organs and tissue engineering. J Membr Sci 308(1–2):1–34
3. Sarwar MS, Niazi MBK, Jahan Z, Ahmad T, Hussain A (2018) Preparation and characterization of PVA/nanocellulose/Ag nanocomposite films for antimicrobial food packaging. Carbohyd Polym 184:453–464
4. Zhang Y, Wei S, Hu Y, Sun S (2018) Membrane technology in wastewater treatment enhanced by functional nanomaterials. J Clean Prod 197:339–348
5. Hussain A, Hägg M-B (2010) A feasibility study of CO2 capture from flue gas by a facilitated transport membrane. J Membr Sci 359(1–2):140–148
6. Wang J, Li M, Zhou S, Xue A, Zhang Y, Zhao Y, Zhong J, Zhang Q (2017) Graphitic carbon nitride nanosheets embedded in poly (vinyl alcohol) nanocomposite membranes for ethanol dehydration via pervaporation. Sep Purif Technol 188:24–37
7. Zhang Y, Yang L, Pramoda KP, Gai W, Zhang S (2019) Highly permeable and fouling-resistant hollow fiber membranes for reverse osmosis. Chem Eng Sci 207:903–910
8. George J, Ishida H (2018) A review on the very high nanofiller-content nanocomposites: Their preparation methods and properties with high aspect ratio fillers. Prog Polym Sci 86:1–39
9. Elele E, Shen Y, Tang J, Lei Q, Khusid B, Tkacik G, Carbrello C (2019) Mechanical properties of polymeric microfiltration membranes. J Membr Sci 591:117351
10. González PS, Agostini E, Milrad SR (2008) Comparison of the removal of 2, 4-dichlorophenol and phenol from polluted water, by peroxidases from tomato hairy roots, and protective effect of polyethylene glycol. Chemosphere 70(6):982–989
11. Julinová M, Vaňharová L, Jurča M (2018) Water-soluble polymeric xenobiotics–Polyvinyl alcohol and polyvinylpyrrolidon—and potential solutions to environmental issues: A brief review. J Environ Manage 228:213–222
12. Shojaeiarani J, Bajwa D, Shirzadifar A (2019) A review on cellulose nanocrystals as promising biocompounds for the synthesis of nanocomposite hydrogels. Carbohyd Polym. 216:247–259
13. Butron A, Llorente O, Fernandez J, Meaurio E, Sarasua J-R (2019) Morphology and mechanical properties of poly (ethylene brassylate)/cellulose nanocrystal composites. Carbohyd Polym 221:137–145
14. Nagalakshmaiah M, Nechyporchuk O, El Kissi N, Dufresne A (2017) Melt extrusion of polystyrene reinforced with cellulose nanocrystals modified using poly [(styrene)-co-(2-ethylhexyl acrylate)] latex particles. Eur Polymer J 91:297–306
15. Miao C, Hamad WY (2016) Alkenylation of cellulose nanocrystals (CNC) and their applications. Polymer 101:338–346
16. Houshyar S, Kumar GS, Rifai A, Tran N, Nayak R, Shanks RA, Padhye R, Fox K, Bhattacharyya A (2019) Nanodiamond/poly-ε-caprolactone nanofibrous scaffold for wound management. Mater Sci Eng C 100:378–387
17. Ljungberg N, Cavaillé J-Y, Heux L (2006) Nanocomposites of isotactic polypropylene reinforced with rod-like cellulose whiskers. Polymer 47(18):6285–6292
18. Santos M, Gangoiti J, Llama MJ, Serra JL, Keul H, Möller M (2012) Poly (3-hydroxyoctanoate) depolymerase from Pseudomonas fluorescens GK13: Catalysis of ester-forming reactions in non-aqueous media. J Mol Catal B 77:81–86
19. Seok JM, Oh SH, Lee SJ, Lee JH, Kim WD, Park S-H, Nam SY, Shin H, Park SA (2019) Fabrication and characterization of 3D scaffolds made from blends of sodium alginate and poly (vinyl alcohol). Mater Today Commun 19:56–61
20. Abdulkhani A, Marvast EH, Ashori A, Hamzeh Y, Karimi AN (2013) Preparation of cellulose/polyvinyl alcohol biocomposite films using 1-n-butyl-3-methylimidazolium chloride. Int J Biol Macromol 62:379–386
21. Bober P, Capáková Z, Acharya U, Zasońska BA, Humpolíček P, Hodan J, Hromádková J, Stejskal J (2019) Highly conducting and biocompatible polypyrrole/poly (vinyl alcohol) cryogels. Synth Met 252:122–126
22. Chaabouni O, Boufi S (2017) Cellulose nanofibrils/polyvinyl acetate nanocomposite adhesives with improved mechanical properties. Carbohyd Polym 156:64–70
23. Koteswararao J, Satyanarayana SV, Madhu GM, Venkatesham V (2019) Estimation of structural and mechanical properties of Cadmium Sulfide/PVA nanocomposite films. Heliyon 5(6):e01851
24. Shao C, Kim H-Y, Gong J, Ding B, Lee D-R, Park S-J (2003) Fiber mats of poly (vinyl alcohol)/silica composite via electrospinning. Mater Lett 57(9–10):1579–1584
25. Feng C, Khulbe K, Matsuura T, Tabe S, Ismail AF (2013) Preparation and characterization of electro-spun nanofiber membranes and their possible applications in water treatment. Sep Purif Technol 102:118–135
26. Zeng C, Zhang L, Cheng X, Wang H, Xu N (2008) Preparation and gas permeation of nano-sized zeolite NaA-filled carbon membranes. Sep Purif Technol 63(3):628–633
27. Sabarish R, Unnikrishnan G (2018) PVA/PDADMAC/ZSM-5 zeolite hybrid matrix membranes for dye adsorption: fabrication, characterization, adsorption, kinetics and antimicrobial properties. J Environ Chem Eng 6(4):3860–3873
28. Liang W, Luo Z, Zhou L (2019) Preparation and characterization of the n-HA/PVA/CS porous composite hydrogel. Chin J Chem Eng
29. Bai J, Li Y, Yang S, Du J, Wang S, Zheng J, Wang Y, Yang Q, Chen X, Jing X (2007) A simple and effective route for the preparation of poly (vinylalcohol)(PVA) nanofibers containing gold nanoparticles by electrospinning method. Solid State Commun 141(5):292–295
30. Aadil KR, Mussatto SI, Jha H (2018) Synthesis and characterization of silver nanoparticles loaded poly (vinyl alcohol)-lignin electrospun nanofibers and their antimicrobial activity. Int J Biol Macromol 120:763–767
31. Xu C, Teja AS (2008) Continuous hydrothermal synthesis of iron oxide and PVA-protected iron oxide nanoparticles. J Supercrit Fluids 44(1):85–91
32. Khorasani MT, Joorabloo A, Moghaddam A, Shamsi H, MansooriMoghadam Z (2018) Incorporation of ZnO nanoparticles into heparinised polyvinyl alcohol/chitosan hydrogels for wound dressing application. Int J Biol Macromol 114:1203–1215
33. Kurczewska J, Pecyna P, Ratajczak M, Gajęcka M, Schroeder G (2017) Halloysite nanotubes as carriers of vancomycin in alginate-based wound dressing. Saudi Pharmaceut J 25(6):911–920
34. Oluwasina OO, Olaleye FK, Olusegun SJ, Oluwasina OO, Mohallem ND (2019) Influence of oxidized starch on physicomechanical, thermal properties, and atomic force micrographs of cassava starch bioplastic film. Int J Biol Macromol 135:282–293
35. Goodarzi H, Jadidi K, Pourmotabed S, Sharifi E, Aghamollaei H (2019) Preparation and in vitro characterization of cross-linked collagen–gelatin hydrogel using EDC/NHS for corneal tissue engineering applications. Int J Biol Macromol 126:620–632
36. Yakovlev S, Medved L (2018) Effect of fibrinogen, fibrin, and fibrin degradation products on transendothelial migration of leukocytes. Thromb Res 162:93–100
37. Cho M-J, Park B-D (2011) Tensile and thermal properties of nanocellulose-reinforced poly (vinyl alcohol) nanocomposites. J Ind Eng Chem 17(1):36–40

38. Li W, Wu Q, Zhao X, Huang Z, Cao J, Li J, Liu S (2014) Enhanced thermal and mechanical properties of PVA composites formed with filamentous nanocellulose fibrils. Carbohyd Polym 113:403–410
39. Moon R, Beck S, Rudie A (2013) Cellulose nanocrystals: a material with unique properties and many potential applications. Review Process: Non-Refereed (Other)
40. Wang D (2019) A critical review of cellulose-based nanomaterials for water purification in industrial processes. Cellulose 26(2):687–701
41. Saheb DN, Jog JP (1999) Natural fiber polymer composites: a review. Adv Polym Technol 18(4):351–363
42. Floyd WC III, Baker SE, Valdez CA, Stolaroff JK, Bearinger JP, Satcher JH Jr, Aines RD (2013) Evaluation of a carbonic anhydrase mimic for industrial carbon capture. Environ Sci Technol 47(17):10049–10055
43. Pabby AK, Rizvi SS, Requena AMS (2008) Handbook of membrane separations: chemical, pharmaceutical, food, and biotechnological applications. CRC Press, Boca Raton
44. Satcher J Jr, Baker S, Kulik H, Valdez C, Krueger R, Lightstone FC, Aines R (2011) Modeling, synthesis and characterization of zinc containing carbonic anhydrase active site mimics. Energy Procedia 4:2090–2095
45. Saeed M, Deng L (2016) Carbon nanotube enhanced PVA-mimic enzyme membrane for post-combustion CO2 capture. Int J Greenh Gas Control 53:254–262
46. Joorabloo A, Khorasani MT, Adeli H, Mansoori-Moghadam Z, Moghaddam A (2019) Fabrication of heparinized nano ZnO/poly (vinylalcohol)/carboxymethyl cellulose bionanocomposite hydrogels using artificial neural network for wound dressing application. J Ind Eng Chem 70:253–263
47. Jahan Z, Niazi MBK, Gregersen ØW (2018) Mechanical, thermal and swelling properties of cellulose nanocrystals/PVA nanocomposites membranes. J Ind Eng Chem 57:113–124
48. Bhowmick S, Koul V (2016) Assessment of PVA/silver nanocomposite hydrogel patch as antimicrobial dressing scaffold: Synthesis, characterization and biological evaluation. Mater Sci Eng C 59:109–119
49. Gupta S, Webster TJ, Sinha A (2011) Evolution of PVA gels prepared without crosslinking agents as a cell adhesive surface. J Mater Sci 22(7):1763–1772
50. Galdeano M, Grossmann M, Mali S, Bello-Perez LA, Garcia M, Zamudio-Flores P (2009) Effects of production process and plasticizers on stability of films and sheets of oat starch. Mater Sci Eng C 29(2):492–498
51. Luo X, Li J, Lin X (2012) Effect of gelatinization and additives on morphology and thermal behavior of corn starch/PVA blend films. Carbohyd Polym 90(4):1595–1600
52. Favier V, Canova G, Cavaillé J, Chanzy H, Dufresne A, Gauthier C (1995) Nanocomposite materials from latex and cellulose whiskers. Polym Adv Technol 6(5):351–355